ACS Catalysis

RESEARCH ARTICLE

pubs.acs.org/acscatalysis

Fischer−Tropsch Synthesis: Characterization and Reaction Testing of Cobalt Carbide

Janet Chakkamadathil Mohandas,[†] Muthu Kumaran Gnanamani,[†] Gary Jacobs,[†] Wenping Ma,[†] Yaying Ji,[†] Syed Khalid,[‡] and Burtron H. Davis*[,†]

[†]Center for Applied Energy Research, University of Kentucky, 2540 Research Park Drive, Lexington, Kentucky 40511, United States

[‡]Brookhaven National Laboratory, 75 Brookhaven Avenue, Upton, New York 11973-5000, United States

ABSTRACT: Hydrogenation of carbon monoxide was investigated for cobalt carbide synthesized from Co_3O_4 by CO carburization in a fixed-bed reactor. The cobalt carbide synthesized was characterized by BET surface area, X-ray diffraction, scanning electron microscopy, X-ray absorption near edge spectroscopy, and extended X-ray absorption fine structure spectroscopy. The catalysts were tested in the slurry phase using a continuously stirred tank reactor at $P = 2.0$ MPa, $H_2/CO = 2:1$ in the temperature range of 493−523 K, and with space velocities varying from 1 to 3 Nl h^{-1} g_{cat}^{-1}. The results strongly suggest that a fraction of cobalt converts to a form with greater metallic character under the conditions employed. This was more pronounced on a Fischer−Tropsch synthesis run conducted at a higher temperature (523 versus 493 K).

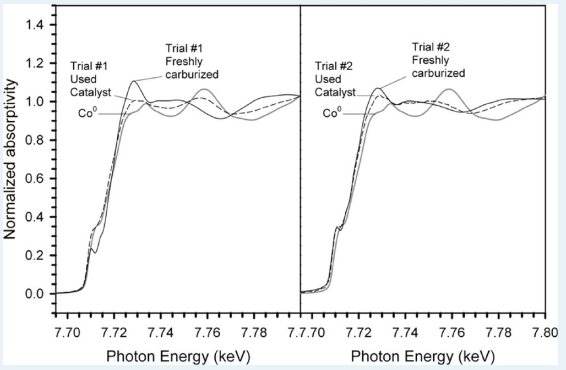

KEYWORDS: carburization, cobalt carbide, cobalt, Fischer−Tropsch synthesis, XANES, EXAFS

1. INTRODUCTION

Fischer−Tropsch (FT) synthesis produces clean hydrocarbon fuels from syngas. Cobalt and iron are the active transition elements often used in the industry for producing hydrocarbons from syngas at elevated temperatures and pressures. Due to their stability and high hydrocarbon productivity, cobalt catalysts represent the ideal choice for synthesizing long-chain hydrocarbons at moderate temperatures and pressures.[1,2] Currently, there is a consensus in the literature that FT synthesis proceeds on cobalt metal particles;[3] nevertheless, a working FT cobalt catalyst could also contain other cobalt species, such as cobalt carbide, cobalt oxides, mixed cobalt-support compounds, etc., which may or may not be directly involved in FT synthesis. Irrespective of conditions employed, however, as with almost all catalysts, Co-FTS catalysts gradually deactivate with time on-stream. Many theoretical and experimental studies suggested various mechanistic pathways for the deactivation of Co-FTS catalysts, including (a) oxidation of metallic Co and support-compound formation,[4−6] (b) poisoning by contaminants on the metallic cobalt phase,[7,8] (c) sintering of the active cobalt phase,[9] and (d) deposition of carbon on Co metal during FTS.[10,11]

There are a number of ways that carbon may form and interact with a Co catalyst during FT synthesis. The formation and influence of bulk cobalt carbide during FTS has been a subject under scrutiny for many years.[12−14] Earlier work at the Bureau of Mines using Co/ThO_2/Kieselguhr catalysts suggests that bulk cobalt carbide was neither an intermediate nor catalytically active for FTS.[15] Weller et al.[13] demonstrated in the 1940s that a bulk cobalt carbide is neither an intermediate nor a catalytically active substrate during FT synthesis, pointing out that carbiding and subsequent hydrogenation of a carburized catalyst produces a hexagonal close packed (hcp) structure of cobalt. However, in a recent review, Moodley et al.[16] describe the formation and influence of carbon on Co-FTS catalysts and indicated that if bulk carbide forms under FTS conditions, it likely influences both CO conversion and selectivity. Karaca et al.,[17] on the basis of results of an in situ XRD study, claimed that cobalt carbide (Co_2C) is stable under FT synthesis conditions when using Pt-promoted cobalt−alumina catalysts, and the authors reported that the XRD profiles did not indicate any structural changes of the carbidized cobalt in the presence of syngas at 493 K and 20 bar pressure. Thus, it is highly desirable to understand the stability and selectivity of bulk cobalt carbide under realistic FT synthesis conditions and assess the likelihood as to whether bulk cobalt carbide contributes to deactivation and, if it does form, how it influences conversion and selectivity.

In the present study, we performed FT synthesis using cobalt carbide (Co_2C) in a conventional CSTR reactor in the temperature range of 493−523 K and 20 bar pressure. The fresh and spent cobalt carbide catalysts were evaluated by EXAFS and XANES to determine local atomic and electronic structure. The results suggest that a fraction of cobalt carbide can convert to a form possessing sufficient metallic character that it does exhibit FT activity.

Received: May 6, 2011
Revised: July 13, 2011
Published: August 15, 2011

2. EXPERIMENTAL SECTION

2.1. Preparation of Cobalt Carbide. The precursor used for the preparation of cobalt carbide was a commercially available high-purity Co_3O_4 (Alfa Aesar). The carburization of cobalt oxide, Co_3O_4, may involve the following steps:

$$Co_3O_4 + CO \rightarrow 3CoO + CO_2$$

$$2CoO + 4CO \rightarrow Co_2C + 3CO_2$$

In our initial study, trial 1, about 2 g of Co_3O_4, a black crystalline powder, was loaded into a stainless steel reactor (5/16 in. (0.79 cm) i.d., 24 in. (61 cm) long), supported by a layer of glass wool. The reactor was placed in a tubular vertical furnace (Lindberg 55102). A K-type thermocouple was situated directly in the sample bed for temperature measurement. The temperature was raised linearly (Omega ramp and soak programmable temperature controller, controlled to ±1 K) with a down-flow of N_2 at 150 $cm^3\ min^{-1}$ using a 1 °C min^{-1} rate from 283 to 523 K and then switching to CO at a flow rate of 50 $cm^3\ min^{-1}$ and holding at 523 K for 52 h. The furnace was then cooled to room temperature in flowing CO (150 $cm^3\ min^{-1}$) for 12 h and passivated for 48 h in 1% O_2 (v/v), balance He at a flow rate of 30 $cm^3\ min^{-1}$. It was left in flowing He overnight. There was a very small exotherm (~5 K) associated with the passivation, which was deemed complete after the sample had once again returned to room temperature after ~220 min. The reactor was then opened to the atmosphere. The black solid thus obtained was used for further characterization. Then 10 g Co_3O_4 was carburized by maintaining the same space velocity so as to obtain Co_2C catalyst for the Fischer−Tropsch synthesis study using a CSTR. No passivation was performed to ensure that the Co_2C catalyst transferred to the CSTR was not exposed to any oxidizing environment. Later, a second study was carried out—trial 2. A similar set of procedures was repeated to prepare the carbide, but without passivation, to avoid any contamination by using 2 g of Co_3O_4 to obtain Co_2C. The resulting carbide was immersed into Polywax-500 and was used for EXAFS studies. A CSTR run was performed using the same catalyst transfer protocol to prevent exposure to oxygen.

Table 1. Characterization Results (trial 1): Pore Diameter, Pore Volume and Surface Area Calculated from N_2 Adsorption Measurements

carburization time/temp	precursor/ carbide	av pore diam (nm)	pore vol (cm^3/g)	surface area (m^2/g)
	Co_3O_4	7.5	0.004	1.7
25 h, 568 K	CoO	7.5	0.011	3.3
52 h, 523 K	Co_2C	5.5	0.025	9
52 h, 568 K	$Co/C/Co_3C$	4.8	0.052	27

2.2. Characterization. *2.2.1. X-ray Diffraction (XRD) Analysis.* The powder diffractogram of the products obtained after carburization was recorded with a Philips X'Pert diffractometer using monochromatic Cu Kα radiation (λ = 1.5418 Å). XRD scans were taken over the range from 2θ of 10−90° to verify the formation of cobalt carbide. The scanning step was 0.01, the scan speed was 0.0025 s^{-1}, and the scan time per step was 4 s.

2.2.2. BET Surface Area Studies. The surface area, pore volume, and average pore radius of the cobalt carbide and cobalt oxide precursor were measured by BET using a Micromeritics Tri-Star 3000 gas adsorption analyzer system. Approximately 0.35 g of sample was weighed and loaded into a 3/8 in. sample tube. Nitrogen was used as the adsorption gas, and sample analysis was performed at the boiling temperature of liquid nitrogen. Prior to the measurement, the sample was slowly ramped to 433 K and evacuated overnight to ~6.7 Pa. Nitrogen served as the adsorption gas, and sample analysis was performed at 77 K.

2.2.3. Scanning Electron Microscopic (SEM) Analysis. Scanning electron microscopic analysis was performed for carburization products along with the precursor Co_3O_4 using a Hitachi S-4800 instrument operating at variable accelerating voltage 0.5−30 kV (variable at 0.1 kV/step) equipped with a secondary electron detector.

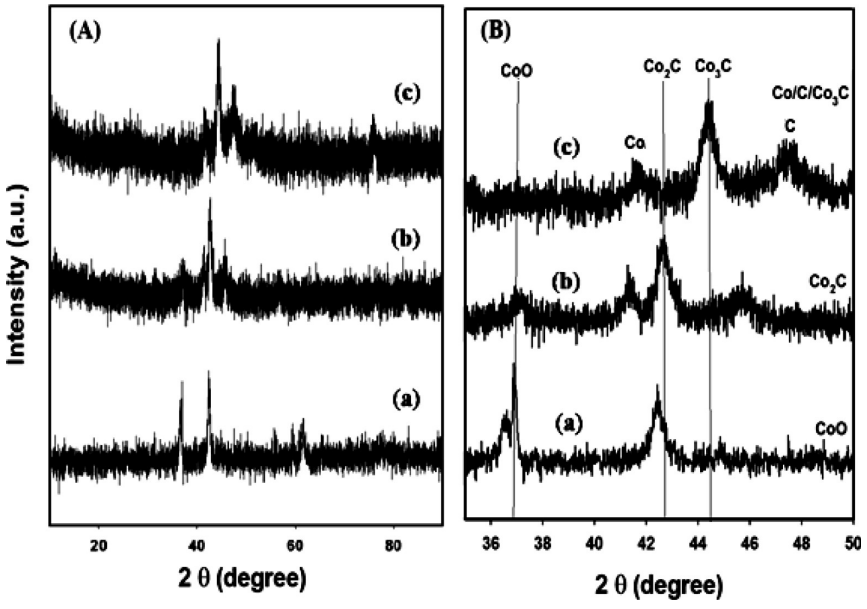

Figure 1. X-ray diffraction patterns for carburization products (trial 1) obtained from Co_3O_4 precursor (A) (a) CoO (25 h, 568 K), (b) Co_2C (52 h, 523 K), and (c) $Co/C/Co_3C$ (52 h, 568 K) and (B) their corresponding magnified portions at 2θ, 35−50°.

dx.doi.org/10.1021/cs200236q |ACS Catal. 2011, 1, 1581–1588

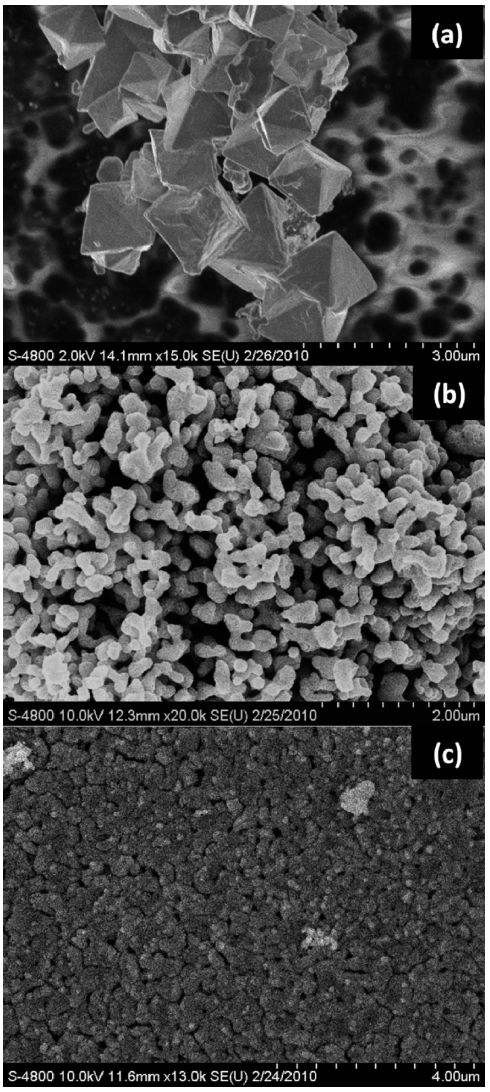

Figure 2. SEM images of (a) Co_3O_4 precursor, (b) Co_2C formed at 523 K, and (c) Co_3C/Co/C formed at 568 K (trial 1).

2.2.4. X-ray Absorption Near Edge Spectroscopy (XANES) and Extended X-ray Absorption Fine Structure (EXAFS) Spectroscopy. The freshly carburized catalysts and the used catalysts following Fischer−Tropsch reaction testing (i.e., sealed in the wax product and indicative of the in situ state) were characterized by XANES and EXAFS spectroscopies at Brookhaven National Laboratory (Beamline X-18b), Upton, New York. EXAFS/XANES spectra were taken in transmission mode.

The beamline is equipped with a Si(111) channel cut monochromator. A crystal detuning procedure was used to help minimize glitches arising from harmonics. The flux at X18b is 1×10^{10} photons/s at 100 mA and 2.8 GeV, and the usable energy range is from 5.8 to 40 keV. Sample thicknesses were estimated by calculating the amount in grams per square centimeter of

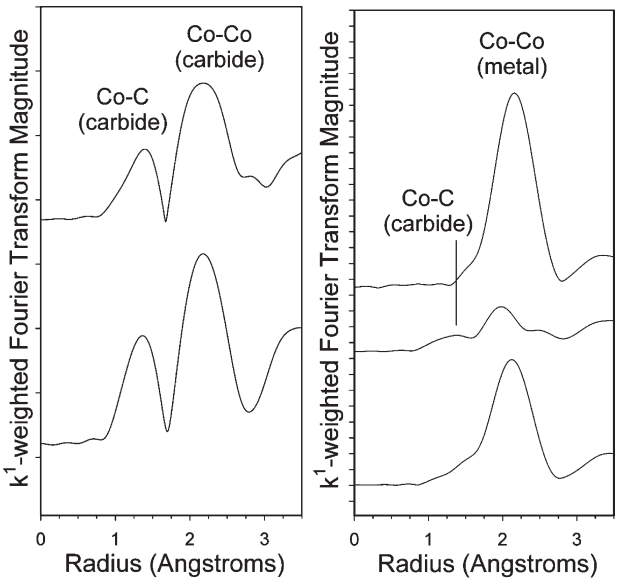

Figure 4. k^1-weighted EXAFS Fourier transform magnitude spectra of the (left) carburized catalysts, including (bottom) trial 1 and (top) trial 2; and (right) used catalysts, including (bottom) the used catalyst for trial 1 and (middle) trial 2, as well as (top) the reference Co^0 foil spectrum.

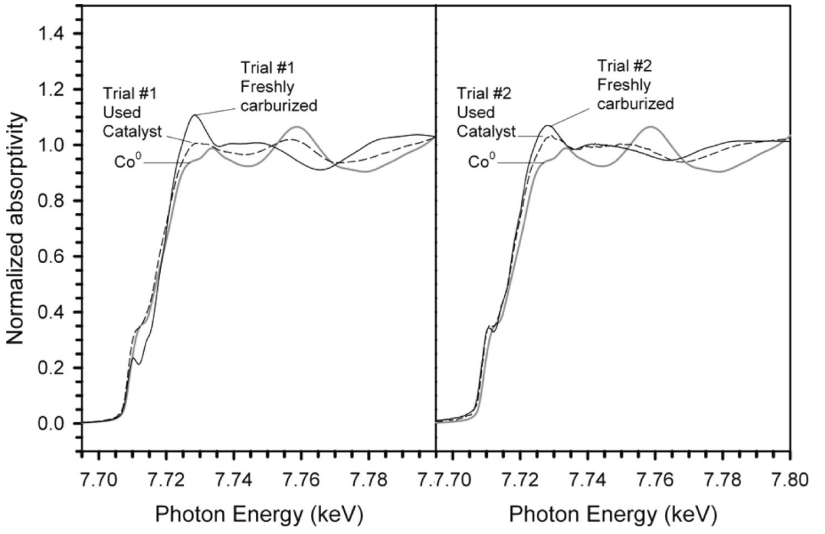

Figure 3. XANES profiles of (thick, dark gray line) Co^0 foil reference, (solid line) freshly carburized catalyst, and (dashed line) used catalyst after running Fischer−Tropsch synthesis.

dx.doi.org/10.1021/cs200236q |*ACS Catal.* 2011, 1, 1581–1588

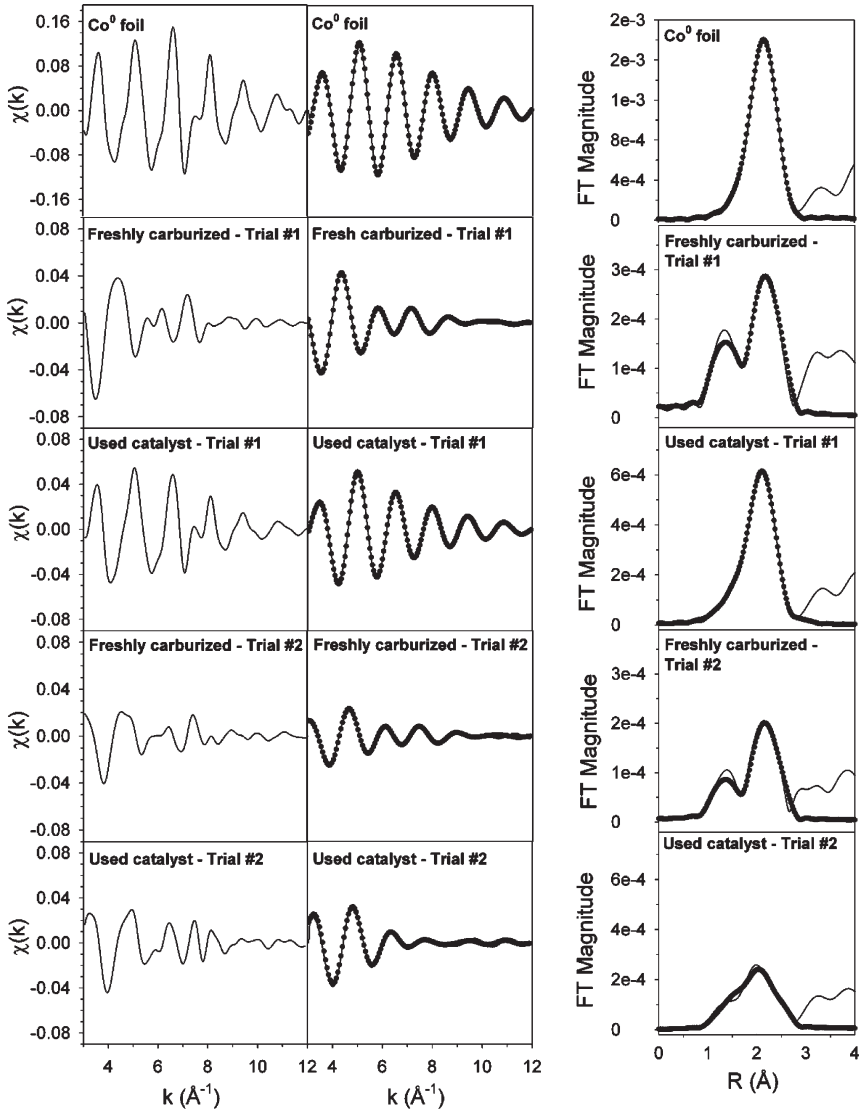

Figure 5. EXAFS results at the Co K-edge for cobalt materials, including (top) cobalt metal foil; (second from top) freshly carburized catalyst, using only Co_2C in the fitting; (middle) the corresponding used catalyst after Fischer−Tropsch synthesis, using both Co_2C and Co^0 in the fitting; (second from bottom) repeat of freshly carburized catalyst, using only Co_2C in the fitting; and (bottom) the corresponding used catalyst after Fischer−Tropsch synthesis, using both the Co^0 metal and Co_2C for fitting. Spectra include (left) the raw $\chi(k)$ versus k, (middle) the filtered $\chi(k)$ versus k and (dotted) the fitting; and (right) the raw Fourier transform magnitude spectrum and (dotted) result of the fitting.

sample, w_D, by utilizing the following thickness equation,

$$w_D = \frac{\ln(I_0/I_t)}{\mathrm{sum}\left\{(m/r)_j w_j\right\}}$$

where m/r is the total cross section (absorption coefficient/density) of element "j" in the sample at the absorption edge of the EXAFS element under study in centimeters squared per gram, w_j is the weight fraction of element j in the sample, and $\ln(I_0/I_t)$ was taken over a typical range of 1−2.5. Smooth, self-supporting pellets of catalyst and wax, free of pinholes, were pressed and scanned. EXAFS data reduction and fitting were carried out using the WinXAS,[18] Atoms,[19] FEFF,[20] and FEFFIT[21] programs. The k and r ranges were approximately 3−12 $Å^{-1}$ and 1.0−2.75 Å. Details of the analysis procedures are reported elsewhere.[22]

2.3. Carbon Monoxide Hydrogenation. The slurry phase reactions were carried out in two runs (trials 1 and 2) in a 1 L CSTR. In each run, ∼8 g of cobalt carbide were transferred into the CSTR reactor from a fixed-bed reactor under the protection of inert N_2. The CSTR was previously charged with 315 g of melted Polywax 3000 as a startup solvent. The carbide catalysts were then activated in situ by flowing carbon monoxide at a space velocity of 3 Nl/g of cat/h at atmospheric pressure and 493 K for 24 h. Following activation, the reactor was cooled to 453 K, and then the reactor pressure was increased to 300 psig using syngas with a H_2/CO molar ratio of 1.93. The reactor temperature was finally ramped to 493 K at 1 °C/min. For trial 1, FT synthesis was performed at two different temperatures, 493 and 523 K, with varying space velocities in the range of 3−1 Nl h^{-1} g^{-1} cat. In a separate independent run (trial 2), a constant reaction temperature of 493 K was maintained throughout the FT synthesis run. Each test was carried out for longer than 300 h.

The gaseous products were analyzed by an online-gas chromatograph (Hewlett-Packard Quad Series Mircro GC).

dx.doi.org/10.1021/cs200236q |ACS Catal. 2011, 1, 1581–1588

Table 2. EXAFS Best Fitting Parameters for Co K-Edge Data[a]

sample description	N Co−C for Co_2C	R Co−C for Co_2C (Å)	N Co−Co for Co_2C	R Co−Co for Co_2C (Å)	e_0 (eV)	σ^2 (Å^2)	r factor
freshly carburized	0.65 (0.0556)	1.924 (0.0154)	0.578 (0.0640)	2.505 (0.0119)	−1.684 (1.145)	0.00442 (0.00167)	0.0046
catalyst, trial 1	1.31 (0.111)	1.930 (0.0154)	0.578 (0.0640)	2.624 (0.0124)			
	total 2.0		2.313 (0.256)	2.629 (0.0125)			
			2.313 (0.256)	2.747 (0.0130)			
			1.157 (0.128)	2.868 (0.0136)			
			total 6.9				
freshly carburized	0.29 (0.0463)	1.862 (0.0252)	0.276 (0.0474)	2.441 (0.0182)	2.847 (1.875)	0.00146 (0.00247)	0.0149
catalyst, trial 2	0.57 (0.0910)	1.868 (0.0252)	0.276 (0.0474)	2.556 (0.0190)			
	total 0.9		1.104 (0.190)	2.562 (0.0190)			
			1.104 (0.190)	2.676 (0.0199)			
			0.552 (0.0948)	2.795 (0.0208)			
			total 3.3				

[a] Ranges used: $\Delta k = 3-12$ Å^{-1} and $\Delta R = 1.0-2.75$ Å. Note: S_0^2 set to 0.90.

Liquid products obtained from hot (373 K) and cold (273 K) traps were combined and then separated into an aqueous phase and a condensed organic liquid phase. Organic products of the Fischer−Tropsch synthesis were analyzed using a gas chromatograph (Hewlett-Packard, HP-5890) equipped with a capillary column DB-5 (length, 60 m; i.d., 0.32 mm; film thickness, 0.25 mm). Helium was used as the carrier gas, and an FID detector was employed and operated with temperature programming from 308 to 598 at 4 K/min. The product data were handled using Hewlett-Packard Chemstation data analysis software.

3. RESULTS

3.1. Characterization. The catalyst compositions and textural properties obtained from N_2 adsorption of the carburized products are given in Table 1. The BET surface area of the carburization product formed after 25 h of carburization by CO was found to be 3 m^2/g, whereas the precursor Co_3O_4 used was ∼2 m^2/g. The BET surface area and pore volume increased with the extent of carburization, and the carburized product obtained after 52 h of carburization at 523 K in the presence of CO was ∼9 m^2/g (trial 1). Carburization for 52 h at 568 K resulted in carbide with a much higher surface area of 27 m^2/g.

XRD patterns of the products (Figure 1A, trial 1) obtained after carburization demonstrate that 25 h of treatment at 568 K resulted in the formation of CoO (JCPDS: 48-1719), indicating that the CO treatment time was not sufficient to complete reduction of Co_3O_4. The product obtained after 52 h of CO treatment at 568 K displayed peaks corresponding to carbon, cobalt, and cobalt carbide (Co_3C), indicating carbon segregation over hexagonal metallic cobalt (JCPDS 5-0727). Carburization for 52 h at 523 K resulted in the formation of bulk cobalt carbide Co_2C (trial 1), as confirmed from JCPDS-5-0704 (Figure 1B) and the profiles did not indicate the presence of any CoO phase having enough long-range order to produce a peak. Although the formal oxidation state of Co in Co_2C is assigned to 2+, in reality, transition metal carbides tend to display significant metallic character.

A scanning electron microscopic image provided in Figure 2a shows octahedral crystallites of Co_3O_4 precursor with a size range of ∼2−4 μm. After carburization for 52 h at 523 K, Co_2C (trial 1) formed, with crystallites ranging from 500 nm to 1 μm in size, as shown in Figure 2b. The octahedral crystallites of Co_3O_4 were etched by the CO gas, removing CO_2 during carburization and resulting in a porous network morphology composed of small crystallites. However, a higher temperature (568 K) treatment for carburization resulted in a similar morphology but with the agglomeration of small crystallites with deposits of carbon located on the surface, as shown in Figure 2c, in agreement with the findings from XRD.

Figure 3 shows the normalized XANES spectra of the Co^0 reference compound and a comparison of the freshly carburized catalyst and the same catalyst after running Fischer−Tropsch synthesis [trial 1(left) and trial 2 (right)]. The line shape of the freshly carburized catalyst differs somewhat from the metal reference compound. The spectrum of the used catalyst, however, appears to exhibit greater metallic character for both runs. Note that a minor contribution to surface oxide cannot be ruled out for the case of trial 1, since the catalyst was passivated after carburization. However, no exposure to oxygen occurred in the case of trial 2. There is a strong resemblance between the spectra of the two freshly carburized catalysts, the main difference being a decrease in the XANES feature close to the edge and perhaps a slightly higher white line in the case of trial 1.

The k^1-weighted EXAFS Fourier transform magnitude spectra are provided in Figure 4. On the left are depicted the carburized catalysts and reveal peaks that, although phase uncorrected, describe the coordination environment around Co. There is a peak at low distance for the first Co−C coordination shells (of which there are two lumped together) and one at higher distance for the first Co−Co coordination shells (of which there are five lumped together). The data suggest that the average particle size may be smaller for the case of trial 2. On the right are the spectra of the used catalysts. In trial 1, the catalyst was exposed to higher temperatures, and a significant peak develops that resembles the Co−Co peak of the metallic foil. In trial 2, during which the temperature was lower, a similar peak begins to develop that is consistent with Co−Co in the metal. It is positioned at a slightly lower distance than that of the peak in trial 1, indicating that the particles may be sufficiently small that some contraction in bond length occurs. However, peaks for the carbide also remain, albeit lower in intensity.

Figure 5 and Tables 2 and 3 provide results of the EXAFS fitting and include the raw, filtered, and fitted $\chi(k)$ spectra, as well as the raw and fitted Fourier transform magnitude spectra of the

dx.doi.org/10.1021/cs200236q |ACS Catal. 2011, 1, 1581–1588

Table 3. EXAFS Best Fitting Parameters for Co K-Edge Data[a]

sample eescription	N Co−C for Co_2C	R Co−C (Å) for Co_2C	N Co−Co metal	R Co−Co (Å) metal	N Co−Co for Co_2C	R Co−Co (Å) for Co_2C	e_0 (eV)	σ^2 (Å^2)	r factor
Co^0 foil			12.0 (set)	2.487 (0.00373)			7.060 (0.4553)	0.00324 (0.000250)	0.00416
used catalyst after Fischer−Tropsch trial 1	0.201 (0.0416)	1.921 (0.00176)	5.0 (0.363)	2.486 (0.00734)	0.201 (0.0416)	2.535 (0.0426)	6.6035 (0.8289)	0.00280 (0.00349)	0.000484
	0.402 (0.0830)	1.927 (0.00177)			0.201 (0.0416)	2.655 (0.0446)	12.2055 (2.737)	0.00468 (0.000701)	
	total 0.6				0.803 (0.166)	2.661 (0.0447)			
					0.803 (0.166)	2.780 (0.0467)			
					0.402 (0.0830)	2.903 (0.0488)			
					total 2.4				
used catalyst after Fischer−Tropsch trial 2	0.238 (0.187)	1.910 (0.0681)	3.0 (6.93)	2.488 (0.159)	0.238 (0.187)	2.548 (0.135)	1.836 (12.051)	0.000001 (0.00648)	0.0128
	0.476 (0.374)	1.916 (0.0683)			0.238 (0.187)	2.669 (0.142)	10.403 (6.889)	0.00931 (0.0187)	
	total 0.7				0.952 (0.748)	2.675 (0.142)			
					0.952 (0.748)	2.794 (0.148)			
					0.476 (0.374)	2.918 (0.155)			
					total 2.8				

[a] Ranges used: $\Delta k = 3-12$ Å^{-1} and $\Delta R = 1.0-2.75$ Å. Note: S_0^2 set to 0.90.

reference Co^0 foil, the two carburized catalysts, and the two used catalysts after carrying out Fischer−Tropsch synthesis. The carburized catalysts exhibit similar oscillation frequencies in the $\chi(k)$ spectra, but differ mainly in the amplitude of the envelope. The $\chi(k)$ spectrum of the used catalyst for trial 1 displays oscillations that more closely resemble those of the Co^0 foil, whereas the spectrum of the used catalyst for trial 2 is intermediate between the spectrum of the carburized catalyst and that of the Co^0 foil.

For the freshly carburized catalyst, a theoretical model generated for Co_2C was found to provide acceptable fits. Again, the smaller values of the coordination numbers for the case of trial 2 may indicate that smaller domains were formed. However, in the case of the used catalysts, the spectra were fitted using a combination of Co^0 metal and Co_2C (i.e., assuming a residual amount of Co_2C remained in the catalyst). In both cases, the coordination of Co−Co in metallic cobalt is significant (i.e., 5.0 and 3.0, respectively, for trials 1 and 2), and the coordination in cobalt carbide has decreased. The results thus suggest that a fraction of the catalyst undergoes transformation from Co_2C carbide to a form of cobalt exhibiting greater metallic character during Fischer−Tropsch synthesis.

3.2. Catalytic Activity. The CO conversion with time-on-stream (TOS) for trials 1 and 2 are shown in Figure 6. In trial 1, cobalt carbide (Co_2C) displayed only 2% CO conversion at 493 K. At this conversion level, the catalyst primarily produced CH_4 and CO_2 (Figure 7). One potential source for the CO_2 is the Boudouard reaction ($2CO \rightarrow C + CO_2$), but evidence to support this is lacking. The detection of CH_4 in the exit gas stream suggests that the initial carburized catalyst had little activity and was selective toward methane under the experimental conditions used. Under the same conditions, the CO conversion slightly increased to 4% after 64 h TOS (Figure 6). Increasing reaction temperature to 523 K increased CO conversion to 12.6% after 104 h TOS. During this period, selectivity for CH_4 and CO_2 stayed constant at 18 and 20%, respectively. A subsequent decrease in space velocity from 3.0 to 1.0 Nl/g of cat/h resulted in an increase in CO conversion to 28.5% after 117 h. The CO conversion remained more or less constant (∼28%) during 117−355 h TOS, indicating that the catalyst exhibited little deactivation.

In trial 2, CO conversion increased to 13% after 70 h of exposure to syngas and remained at this pseudosteady-state conversion of CO for at least 300 h of TOS before the run was terminated. The hydrocarbon products were those expected for low α FT synthesis (Figures 8 and 9). Indeed, both runs yield higher selectivity to methane and CO_2, irrespective of the conditions followed. These results are consistent with an early experimental study over Co_2C reported by Weller et al.[13] and a recent DFT study of cobalt carbides for FTS,[23] which suggests that Co_2C inhibits FTS and is a source of high CH_4 selectivity. Weller et al.[13] have demonstrated that cobalt−thoria−Kieselguhr catalyst was inactive when exposed to synthesis gas at 455 K after carburization at 473 K for 24 h, but the gas contraction increased to 33% with a subsequent increase in the reaction temperature to 463 K. Furthermore, the authors concluded that highly active hcp cobalt was produced by reduction of cobalt carbide under realistic FT synthesis conditions.

3.3. Discussion. Many interesting studies have appeared in the literature about the effect of carbon on hydrocarbon selectivity over cobalt FT catalysts. A recent work at Sasol has shown that even exposure to pure CO for 2 h can be detrimental to CO conversion and selectivity after resuming FT synthesis conditions.[24]

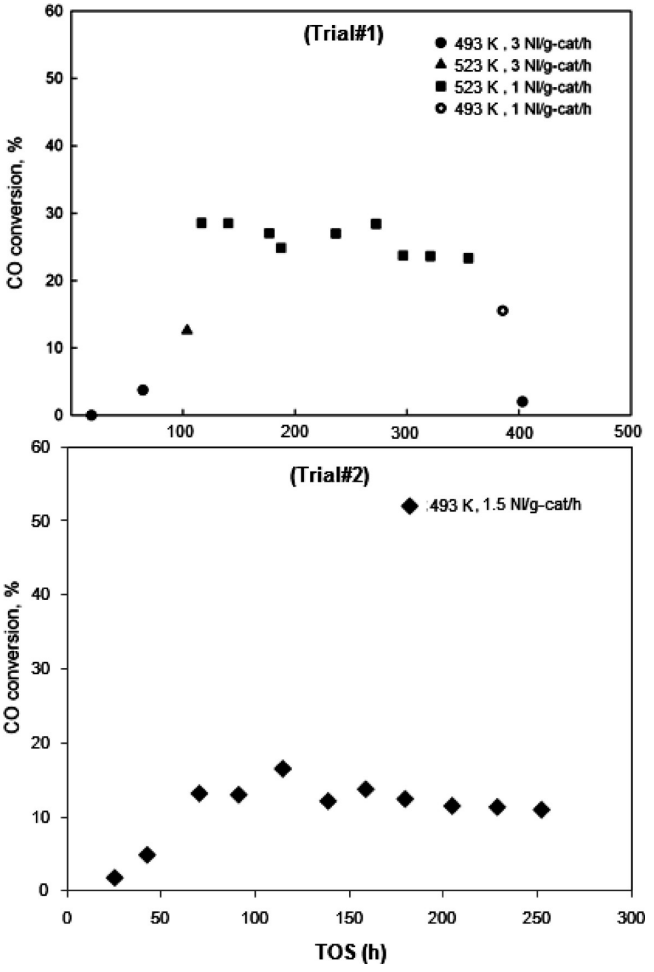

Figure 6. Change of CO conversions with time and reaction conditions over Co_2C catalyst: (top) trial 1 and (bottom) trial 2.

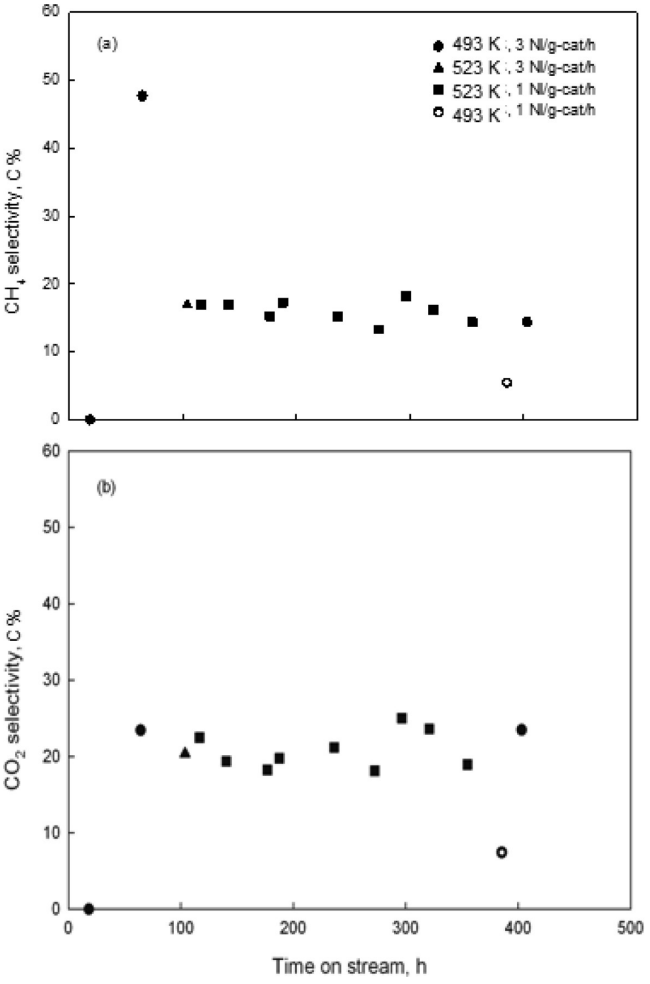

Figure 7. Change of (a) CH_4 and (b) CO_2 selectivities with time and reaction conditions over Co_2C catalyst (trial 1).

In our study, the initial catalytic phase, that is, cobalt carbide (Co_2C), has very low FTS and WGS activity. Despite the very low CO conversion in trial 2, the selectivities to CH_4 and CO_2 were high (i.e., 67% and 33%, respectively). As temperature increased to 523 K, CO conversion increased to 13 (3 Nl/g of cat/h) and 28% (1 Nl/g of cat/h). At the same time, the selectivity to CH_4 decreased to 16%, and heavier organic products started to form (Figure 7), resembling the normal FTS products produced over active Co catalysts, where the active surface is suggested to be Co^o.[25] However, the chain growth probability ($\alpha_{C3-C17} = 0.62$) obtained after 100 h TOS was still well below that of standard Co FTS catalysts (α−0.85−0.89).

It is surprising to see that a drop in CH_4 selectivity to less than 10% occurred with catalyst aging (Figure 7) at the same reaction temperature (493 K). It was reported that carbon in bulk Co_2C can be easily removed through hydrogenation ($Co_2C + H_2 \rightarrow Co + CH_4$) within several hours, even within a low temperature range 423−467 K.[13] However, the authors did not mention if this phase transition could occur under FT synthesis conditions. Unlike the unsupported bulk cobalt carbide used in our system, Khodakov et al.[17,26] recently showed, using alumina-supported cobalt catalyst, that cobalt carbide is likely to form via carbiding metallic cobalt. They concluded that sintering and carburization of cobalt at longer lengths of time on stream could be responsible for the deactivation of alumina-supported cobalt catalysts. It is difficult to understand why the alumina support should modify the cobalt carbide to such an extent that the metal should carbide during FT synthesis.

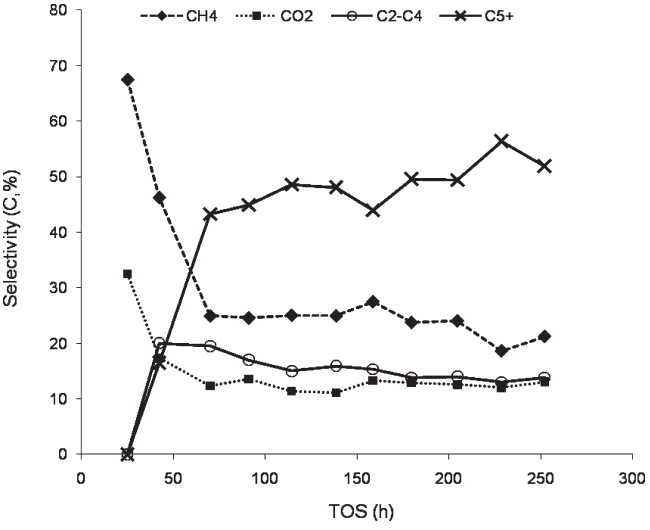

Figure 8. Change of selectivity with time-on-stream for FT synthesis of Co_2C catalyst at 493 K, 300 psig, and SV of syngas 1.5 Nl/g of cat/h (trial 2).

dx.doi.org/10.1021/cs200236q |ACS Catal. 2011, 1, 1581–1588

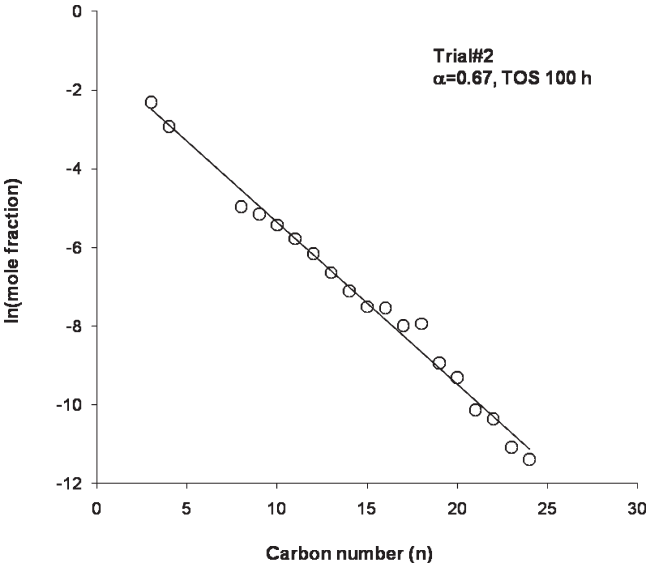

Figure 9. ASF plot showing the FT product distribution for the trial 2 catalyst.

In our system, cobalt carbide Co_2C tends to form metallic Co during Fischer−Tropsch synthesis at 493−523 K and produce higher hydrocarbons. In general, a typical cobalt FT catalyst shows only very low water−gas shift activity under FT synthesis conditions; however, in this system, we have obtained more CO_2 at two different synthesis conditions (493 and 523 K), and this is probably due to the simultaneous presence of Co_2C along with a form of cobalt exhibiting greater metallic character, as evidenced from EXAFS and XANES.

4. CONCLUSIONS

Cobalt carbide, Co_2C, was synthesized by carburization of cobalt oxide Co_3O_4 in CO and characterized using BET surface area, X-ray diffraction, scanning electron microscopy, X-ray absorption near edge spectroscopy, and extended X-ray absorption fine structure spectroscopy. The X-ray diffraction pattern of the freshly carburized cobalt catalyst at 523 K reveals the formation of the Co_2C phase. XANES and EXAFS results of fresh and used catalysts indicate that a fraction of the Co_2C reduced to a form of cobalt that was active under FT synthesis conditions. The initial FTS activity over bulk cobalt carbide yielded mostly methane and CO_2, but as time progressed, CO conversion as well as the selectivity to higher hydrocarbons increased. The α value obtained after 100 h TOS shows the chain growth probability of the catalyst increases with decreasing carbide content. Bulk cobalt carbide appears to be unstable under FTS conditions, especially at higher reaction temperatures.

AUTHOR INFORMATION

Corresponding Author

*Phone: 859-257-0251. Fax: 859-257-0302. E-mail: burtron.davis@uky.edu.

ACKNOWLEDGMENT

This work was supported by the Commonwealth of Kentucky. A part of the research was carried out at the National Synchrotron Light Source, Brookhaven National Laboratory, which is supported by the U.S. DOE, Divisions of Materials Science and Chemical Sciences.

REFERENCES

(1) Khodakov, A. Y.; Chu, W.; Fongarland, P. *Chem. Rev.* **2007**, *107*, 1692–1744.
(2) Jager, B.; Espinoza, R. *Catal. Today* **1995**, *23*, 17–28.
(3) Iglesia, E.; Reyes, S. C.; Madon, R. J.; Soled, S. L. *Adv. Catal.* **1993**, *39*, 221–302.
(4) van Berge, P. J.; van de Loosdrecht, J.; Barradas, S.; van der Kraan, A. M. *Catal. Today* **2000**, *58*, 321–334.
(5) Jacobs, G.; Das, T. K.; Patterson, P. M.; Li, J.; Sanchez, L.; Davis, B. H. *Appl. Catal., A* **2003**, *247*, 335–343.
(6) Hilmen, A. M.; Schanke, D.; Hanssen, K. F.; Holmen, A. *Appl. Catal., A* **1999**, *186*, 169–188.
(7) Bartholomew, B. H. *Appl. Catal., A* **2001**, *212*, 17–60.
(8) Rostrup-Nielsen, J. R. In *Catalysis Science and Technology*; Anderson, J. R., Boudart, M., Eds.; Springer-Verlag: Berlin, 1984; p 1.
(9) Kiss, G.; Kliewer, C. E.; DeMartin, G. J.; Culross, C. C.; Baumgartner, J. E. *J. Catal.* **2003**, *217*, 127–140.
(10) Lee, D. K.; Lee, J.-H.; Ihm, S.-K. *Appl. Catal.* **1988**, *36*, 199–207.
(11) Gruver, V.; Young, R.; Engman, J.; Robota, H. J. *Prepr.—Am. Chem. Soc. Div. Pet. Chem.* **2005**, *50*, 164–166.
(12) Gruver, V.; Zhan, X.; Engman, J.; Robota, H. J.; Suib, S. L.; Polverejan, M. *Prepr.—Am. Chem. Soc. Div. Pet. Chem.* **2004**, *49*, 192–194.
(13) Weller, S.; Hofer, L. J. E.; Anderson, R. B. *J. Am. Chem. Soc.* **1948**, *70*, 799–801.
(14) Hofer, L. J. E.; Cohn, E. M.; Peebles, W. C. *J. Phys. Colloid Chem.* **1949**, *53*, 661–669.
(15) U.S. Bureau of Mines. *Bulletin 578*; U.S. Government Print Office: Washington, DC, 1948−1959; http://www.fischer-tropsch.org.
(16) Moodley, D. J.; van de Loosdrecht, J.; Saib, A. M.; Niemantsverdriet, J. W. In *Advances in Fischer−Tropsch Synthesis, Catalysts and Catalysis*; Davis, B. H., Occelli, M. L., Eds.; Taylor & Francis: Boca Raton, FL, 2009; p 49.
(17) Karaca, H.; Safonova, O. V.; Chambrey, S.; Fongarland, P.; Roussel, P.; Griboval-Constant, Z.; Lacroix, M.; Khodakov, A. Y. *J. Catal.* **2011**, *277*, 14–26.
(18) Ressler, T. *WinXAS 97, Version 1.0*; 1997.
(19) Ravel, B. *J. Synchrotron Radiat* **2001**, *8*, 314–316.
(20) Rehr, J. J.; Zabinsky, S. I.; Albers, R. C. *Phys. Rev. Lett.* **1992**, *69*, 3397–3400.
(21) Newville, M.; Ravel, B.; Haskel, D.; Stern, E. A.; Yacoby, Y. *Phys. B* **2005**, *208−209*, 154–156.
(22) Jacobs, G.; Sarkar, A.; Ji, Y.; Luo, M.; Dozier, A.; Davis, B. H. *Ind. Eng. Chem. Res.* **2008**, *47*, 672–680.
(23) Cheng, J.; Hu, P.; Ellis, P.; French, S.; Kelly, G.; Lok, C. M. *J. Phys. Chem. C* **2010**, *114*, 1085–1093.
(24) Moodley, D. J. Ph.D. thesis, Eindhoven University of Technology, The Netherlands, 2008.
(25) Iglesia, E. *Appl. Catal., A* **1997**, *161*, 59–78.
(26) Karaca, H.; Hong, J.; Fongarland, P.; Roussel, P.; Griboval-Constant, A.; Lacroix, M.; Hortmann, K.; Safonova, O. V.; Khodakov, A. Y. *Chem. Commun.* **2010**, *46*, 788–790.